applied sciences

MDPI

Article

Design and Numerical-Method-Aided Optimization of a Novel Attachment System for Implant-Retained Dental Prostheses Using NiTi Shape Memory Alloys

Pejman Shayanfard [1,2], Frank Wendler [1], Philipp Hempel [3] and Matthias Karl [4,*]

[1] Institute of Materials Simulation, Friedrich-Alexander University of Erlangen-Nürnberg, 90762 Fürth, Germany
[2] Department of Functional Materials, Institute of Physics of the Czech Academy of Sciences, 18221 Prague, Czech Republic
[3] ADMEDES GmbH, 75179 Pforzheim, Germany
[4] Department of Prosthodontics, Saarland University, 66424 Homburg, Germany
* Correspondence: matthias.karl@uks.de

Abstract: While nickel-titanium (NiTi) is the primary shape memory alloy (SMA) used in endodontic instruments, restorative dental components so far have not been fabricated from SMAs. The flexibility of these materials may solve problems in implant prosthodontics resulting from non-parallel implant positions and transfer inaccuracies. Based on a prototype of a novel attachment system for implant overdentures, a finite element model was created and used for studying different loading situations and design parameters followed by numerical analysis aided design optimization. The results revealed that the basic design of the attachment is capable of compensating misalignments of supporting implants as well as transfer inaccuracies of a clinically relevant magnitude by accommodating the large deformations induced under masticatory loading upon martensitic phase transformation at almost constant stress. The application of NiTi resulted in the reduction of the reaction forces recorded in the surrounding of the supporting implant, as well, the reaction forces between male and female parts of the attachment system could be reduced which will minimize wear phenomena and subsequent maintenance costs. These effects were seen to be enhanced in the optimized design.

Keywords: dental prosthesis; implant-supported; denture precision attachment; finite element analysis; shape memory alloys

Citation: Shayanfard, P.; Wendler, F.; Hempel, P.; Karl, M. Design and Numerical-Method-Aided Optimization of a Novel Attachment System for Implant-Retained Dental Prostheses Using NiTi Shape Memory Alloys. *Appl. Sci.* **2023**, *13*, 491. https://doi.org/10.3390/app13010491

Academic Editor: Vittorio Checchi

Received: 18 November 2022
Revised: 21 December 2022
Accepted: 28 December 2022
Published: 30 December 2022

1. Introduction

Nickel-Titanium (NiTi) shape memory alloys (SMAs) belong to the group of metallic alloys known as smart functional materials. Their functional behaviors cover mainly superelasticity, shape memory effect, and shape memory actuation. Superelasticity is related to the cyclic recovery of large thermo-elastic transformation strains on unloading, the shape memory effect is correlated to the recovery of large thermo-elastic transformation strains upon heating, and shape memory actuation describes the cyclic recovery of large thermo-elastic transformation strain upon heating under an external bias load [1,2]. The superelastic property of NiTi shape memory alloys is based on the induction of phase transformation during mechanical loading and has recently been shown to arise from its microstructure [3]. Their promising biocompatibility [4] allows for applications in the design of many novel biomedical devices and implants [5–7]. Prior to entering costly prototype fabrication for such novel applications, Finite element analyses could enhance understanding of their physical responses under biomedical loading scenarios [8–10]. A novel application for NiTi may be seen in dental implant prosthodontics for compensating shortcomings with respect to the parallelism of supporting implants as well as transfer inaccuracies between the patient situation and the laboratory working cast.

The use of two dental implants in the interforaminal region and corresponding attachments for stabilizing complete dentures (Figure 1) is a frequently applied [11] and cost-effective treatment option [12], which is well documented in the literature.

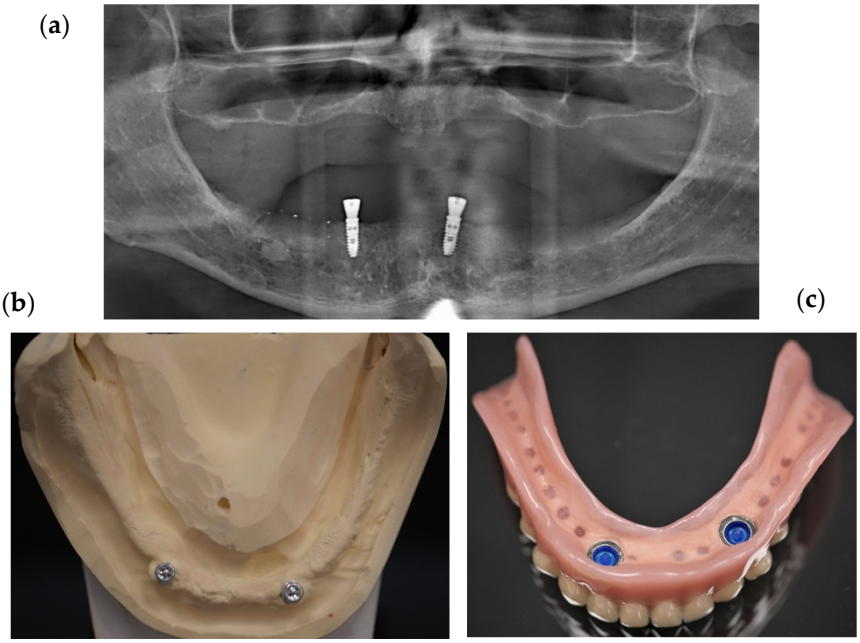

Figure 1. (**a**) Panoramic X-ray of an edentulous patient with two interforaminal implants showing a distinct inter-implant angulation, (**b**) Mandibular cast of the patient shown in Figure 1a with two male Locator attachments in place, (**c**) Removable prosthesis with female parts of the Locator attachment system.

The use of prefabricated attachment systems such as locators (Zest Dental Solutions, Carlsbad, CA, USA), instead of utilizing individually fabricated attachments such as telescopic crowns or bars, drastically reduces the initial treatment costs in the edentulous mandible [13,14]. Several studies have shown that maintenance frequency [15] and associated costs [16] in such restorations are quite high, equaling or even exceeding initial treatment fees [14,17]. In particular, loss of retention and fractures of the prostheses in the area of the attachment constitute the two main technical complications [18,19].

From a biomechanical perspective, the non-parallelism of supporting implants and transfer inaccuracies between the clinical and the laboratory situation may be seen as major reasons for wear phenomena occurring at the retentive interface of the attachment system [20,21]. This assumption is supported by clinical studies showing that inter-implant angulation resulted in a greater amount of wear of the attachments used [22,23]. Two in vitro studies showed that retentive forces deteriorated faster when the attachments were supported by angulated implants as compared to implants with a strictly parallel orientation [24,25]. Coatings of the male attachment parts [22], as well as the use of different plastic inserts in the female parts, seemed to have only a minor effect on wear phenomena. Compromised clinical results have been reported for maxillary full arch restorations supported by two to four implants arguing that potentially detrimentally high levels of moment loading transferred via a stiff attachment system were a co-factor in these cases [26,27].

To compensate for the non-parallelism of implants and transfer inaccuracies, as well as to avoid excessive moment loading of supporting implants under dynamic masticatory loading, an attachment system has recently been described [28] incorporating a superelastic Nickel-Titanium (NiTi) element (Figures 2 and 3). The form of the NiTi element resembling the shape of an endodontic instrument [29] is supposed to allow for lateral flexibility of

the male part of the attachment while axial loads shall be transferred to the implant and surrounding bone.

Figure 2. Prototype attachment consisting of a base fixed on a tissue-level titanium dental implant with a rod-shaped connector extending from the base to a retentive structure onto which a removable prosthesis can be mounted (here formed as a cylindrical telescopic crown).

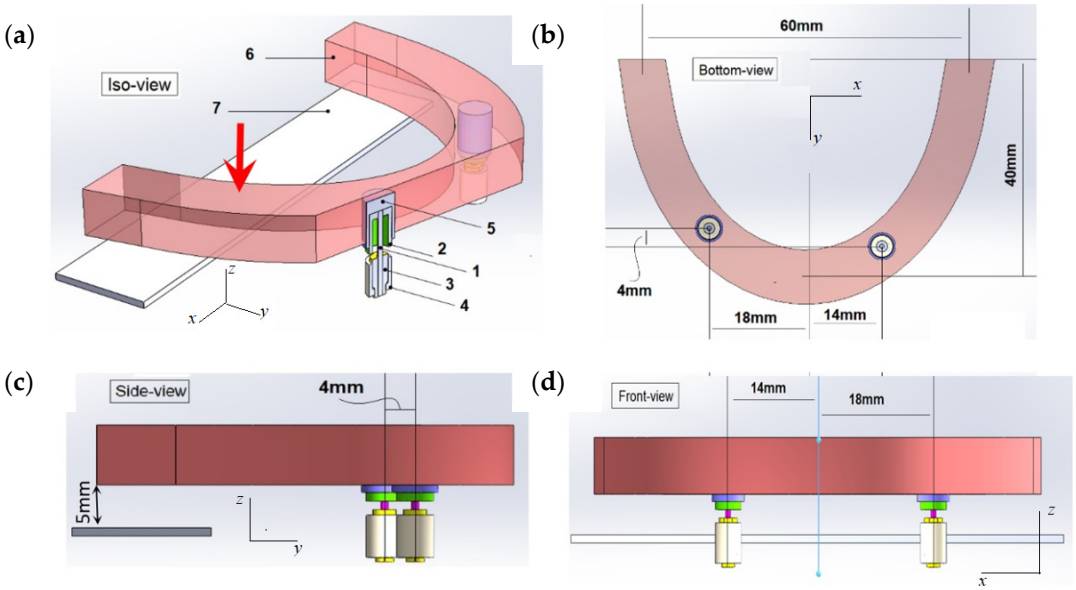

Figure 3. (**a**) Iso view of the reference model based on a patient situation and prototype attachment represented in Figures 1 and 2, representing the ideal parallel positioning of the two supporting implants. The single components of the attachment system were: 1—NiTi shaft of the male part of the attachment, 2—NiTi head of the male part of the attachment, 3—NiTi abutment of the male part of the attachment, 4—tissue-level dental titanium implant, 5—female part of the attachment system, 6—removable prosthesis with female parts of the attachment system, 7—stiff plate simulating the patient's soft tissue limiting the maximum vertical displacement of the removable prosthesis caused by masticatory loading to 5 mm; bottom view (**b**), side view (**c**), and front view (**d**) of the reference model.

It was the goal of this optimization study to analyze the behavior of a flexible attachment system made of superelastic NiTi alloy and allow for lateral and angular flexibility under the multiaxial loads induced by a moving prosthesis upon masticatory loading.

2. Materials and Methods

2.1. Design and Prototype Manufacturing

The design of the male attachment part is shown in Figures 2 and 3 detailing the description of its components. This attachment system (in a previous prototype stage) has been used for an in vitro biomechanical study [28] and consisted of assembled NiTi superelastic components which all conform with ASTM F2633. A NiTi wire with a principal diameter of 0.8 mm was welded at the top to a one-sided closed tube and the bottom to a base. The upper tube end was closed by welding a cylindrical hole plate on it with the same diameter as the outer diameter of the tube. The diameter of the hole in the plate was slightly larger than the wire diameter for ease of welding. At the bottom, the wire was welded to the base in order to increase stability against damage to the welding joint at large shear forces. An outer thread was machined at the bottom of the base so that the attachment system could be mounted on a titanium dental implant. Although it would not have been necessary for the mechanical performance of the device to use only NiTi for all components, it was necessary for the welding process due to issues with the welding of dissimilar metals involving NiTi. Heat treatment was only necessary for the wire to adjust the functional Af temperature to 17 $\pm$ 5 °C so that the mechanical behavior was superelastic at body temperature.

2.2. Finite Element Simulation Method

In order to analyze the mechanical response of the NiTi superelastic male attachment part the evolution of the martensite phase fraction and local stress magnitude under multiaxial loading occurring as a consequence of mastication seemed to be important. To that end, a three-dimensional mathematical phenomenological SMA model proposed by Choudhry and Yoon [30], which has also been numerically implemented in the MSC Marc finite element software and which has also been comprehensively outlined in the supplementary material of Ref [31] was used. This model's capabilities include capturing phase transformation between the austenite and martensite phases, as well as the tension-compression asymmetry in SMAs by the Conical Drucker approach.

The reference geometric model shown in Figure 3a consisted of the male part of the attachment made of NiTi superelastic alloy, a stiff removable prosthesis with female attachment parts, and a titanium implant. The model was generated based on an existing patient situation (Figure 1) and the dimensions of the prototype of the attachment system (Figure 2). In all simulations, a unilateral vertical force of 150 N was applied on a few nodes resembling the approximated molar region of the prosthesis (red arrow in Figure 3a). Prosthesis displacement under masticatory forces was considered the standard cyclic loading scenario the attachment has to withstand during function. While prosthesis displacement should clinically be kept as low as possible e.g., by relining, 5 mm of vertical displacement in the posterior region of the prosthesis was chosen for simulating a worst-case scenario. To this end, a stiff plate was modeled at the posterior end of the prosthesis and fixed at the bottom (see component number 7 in Figure 3a,c). Elastic deformation of alveolar bone as a result of loading was not of primary interest here but instead, all degrees of freedom at the outer surface of the dental implant were fixed.

Positional discrepancies between male and female parts of the attachment systems constitute a frequent clinical problem and result from non-parallelism of implants and transfer inaccuracies during prosthesis fabrication. Accordingly, the FE analysis of the reference design (following the prototype) with parallel alignment of the supporting implants (Figure 3) was compared to the situation of the non-parallelism of the supporting implants (Figure 4). For design optimization, two alternative designs of the male attachment part were examined representing a larger contact area between the shaft and the male retentive element and a necked shaft, respectively (Figure 5). Furthermore, a case study with the male part made purely from titanium was investigated for comparison.

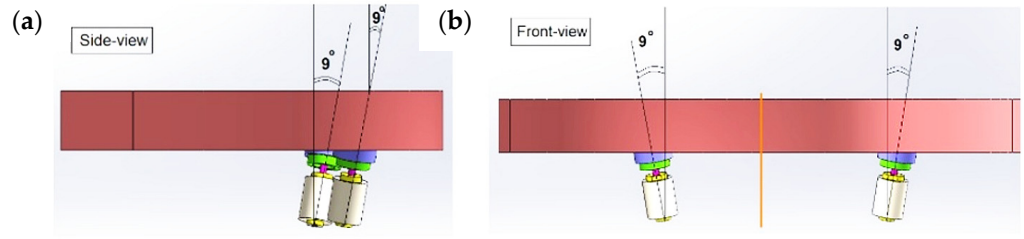

Figure 4. Non-parallel positioning of two supporting implants. Approximately nine degrees axial deviation in two axes were considered for both supporting implants, (**a**) side view, and (**b**) front view.

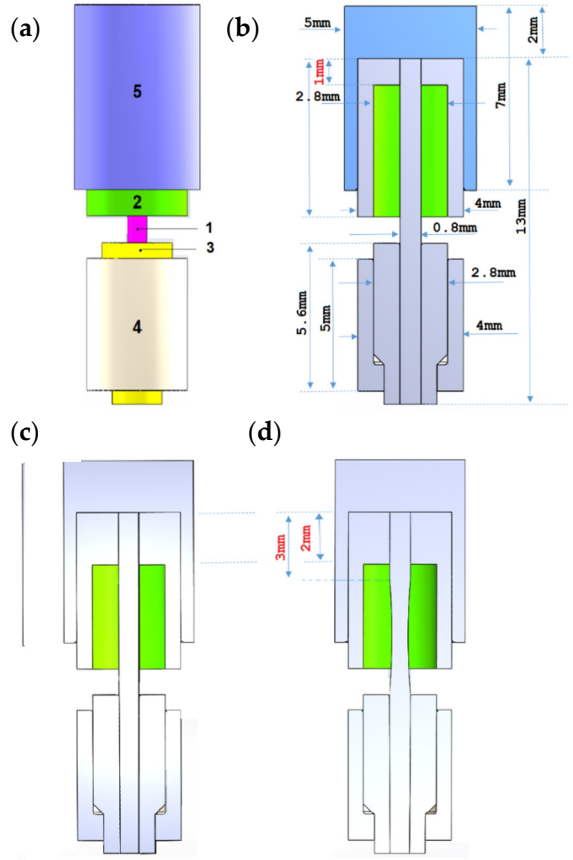

Figure 5. Details, dimensions, and cross-section exhibition of the NiTi male part (the description of each numbered component can be found in Figure 3): (**a**,**b**) the reference geometric design created based on the prototype shown in Figure 2, (**c**) the alternative design 1 where the contact area between the shaft and male attachment part was increased from 1 mm to 2 mm, (**d**) the alternative design 2 where—additionally to changes described in 'c'—the shaft was necked in the middle by reducing the 0.8 mm overall diameter to 0.6 mm.

The material properties for the shape memory NiTi wire (part 1 in Figures 3 and 5) determine the superelastic response of the device. In the present simulations, transformation temperatures M_s, M_f, A_s, A_f, austenite and martensite elastic moduli EA and EM, Poisson ratio ν_A and ν_M, thermal stress influences coefficients C_A and C_M and transformation strain ϵ_{eq}^T were adapted to tensile experimental data obtained by the manufacturer of the prototype NiTi attachment (ADMEDES GmbH, Pforzheim, Germany) which are given in Figure 6 and in Table 1. It should be noted that, since the experimental data for the tensile test was available only at a single temperature, the fitting parameters including the transformation temperatures could be unrealistic compared to those of the commercial NiTi used in medical devices. Nevertheless, this approach still satisfied the fitting to the mechanical re-

sponse of the device at the studied temperature in the present work. A tension-compression asymmetry of the moduli and stress plateaus in the order of typical reported values [32,33] was assumed (Figure 6). The quantities g_a in Table 1 parametrize an empiric function describing the level of alignment of transformation strain and deviatoric stress (see supplementary material in [30]). The mechanical properties of Ti-30%Au alloy [34] were used for simulating the female attachment part (number 5 in Figures 3a and 5).

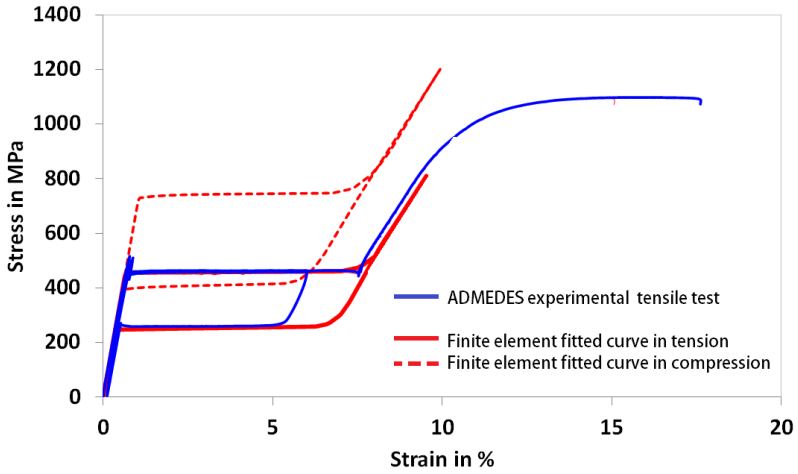

Figure 6. The uniaxial mechanical response obtained by fitting parameters of the FEM model to the experimental results recorded by the manufacturer of the prototype NiTi attachment system (ADMEDES GmbH, Pforzheim, Germany), and considering the assumed tension-compression asymmetry [32,33].

Table 1. Material parameters of the SMA constitutive model, for more details, refer to supplementary material in ref [30].

				g **Function (Fitting) Parameters**			
Param./[Unit]	g_a [-]	g_b [-]	g_c [-]	g_d [-]	g_e [-]	g_f [-]	g_0 [MPa]
Values	−2	2	0	2.75	0	3	300
Param./[unit]	M_s [°C]	M_f [°C]	A_s [°C]	A_f [°C]	C_M [MPa/°C]	C_A [MPa/°C]	
Values	−63	−65	−13	−10	5.45	6.25	
Param./[unit]	E_M [GPa]	E_A [GPa]	ν_M [-]	ν_A [-]	ϵ_{eq}^T [-]		
Values	19	61	0.33	0.33	0.049		

In the FEM method, a glue-segment-to-segment contact was used at all contact surfaces, except for the contact between components number 6 and 7 (Figures 3a and 5) where sliding contact with bilinear friction force tolerance of 0.1 has been used.

3. Results

The major mode of deformation induced by the masticatory force F (Figures 3a and 7) was bending, leading to compressive- and tensile-loaded zones of the NiTi shaft. The surfaces at the SMA shaft where compressive stresses were dominant were named oral according to their location in the oral cavity (right patient side: O_1; left patient side: O_2), while the opposite sides were associated with tensile stresses and named buccal (right patient side: B_1; left patient side: B_2) (Figure 7).

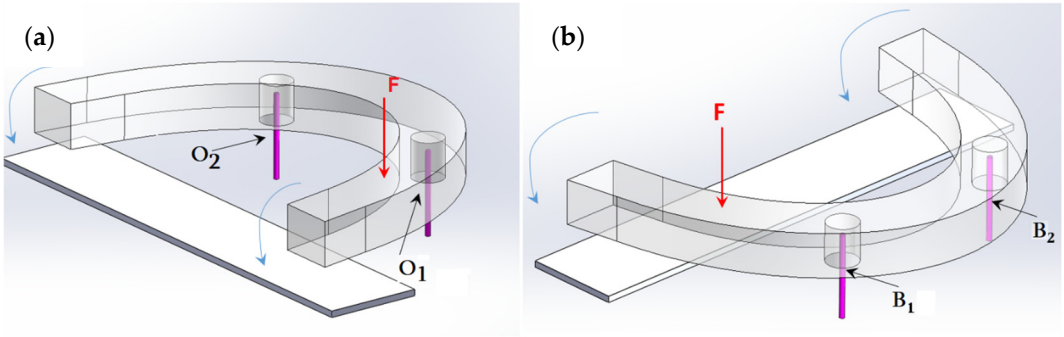

Figure 7. (**a**) Iso view of the FE model showing the SMA shaft (purple) with bending-induced zones (**a**) O_1 and O_2 dominated by compressive stresses (at *Oral Surface*), (**b**) B_1 and B_2 dominated by tensile stresses (at *Buccal Surface*).

Force application in rising magnitude resulted in two subsequent stages of deformation. In the first stage, it caused a maximum vertical displacement of 5 mm at the posterior end of the prosthesis until mechanical contact with the binding sheet (Figure 8). In this stage, the dominant deformation observed was the bending of the SMA shafts. In the course of contact, at the second stage, the continuation of the loading induced compressive stresses on the SMA shafts.

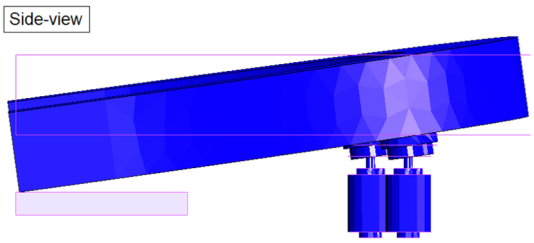

Figure 8. Vertical prosthesis displacement at the posterior border was limited to 5 mm by simulating a binding sheet.

The surface distribution of the axial stresses and martensite volume fractions at maximum load for all studied geometries (parallel and non-parallel implant fixation for prototype abutment design, as well as the non-parallel fixation for the optimized/alternative designs) are given in Figure 9. Throughout this section, the term axial denotes the z direction of the reference cartesian system (Figure 3). Here, the SMA material is used for the male part, shaft, and base parts. Figure 9(a1–d1) show the axial stress at surfaces that are dominantly under compressive stresses (Oral Surfaces) and denoted by O_1 and O_2, while in Figure 9(a2–d2,a3–d3) their corresponding axial strain and volume fraction of detwinned martensite are depicted, respectively.

In contrast, Figure 9(a4–d4) exhibit the axial stress distribution at Buccal Surfaces (denoted by B_1 and B_2), and their associated strains and martensite volume fractions are represented in Figure 9(a5–d5) and Figure 9(a6–d6), respectively. In Figure 10 the corresponding stress-strain responses at representative points (maximum martensite fraction points) at Oral and Buccal surfaces from Figure 9a–d are represented. For comparative purposes, Figure 11 represents the case study in which the material for the SMA parts was replaced by titanium (in the non-parallel fixation case study, see Figure 4).

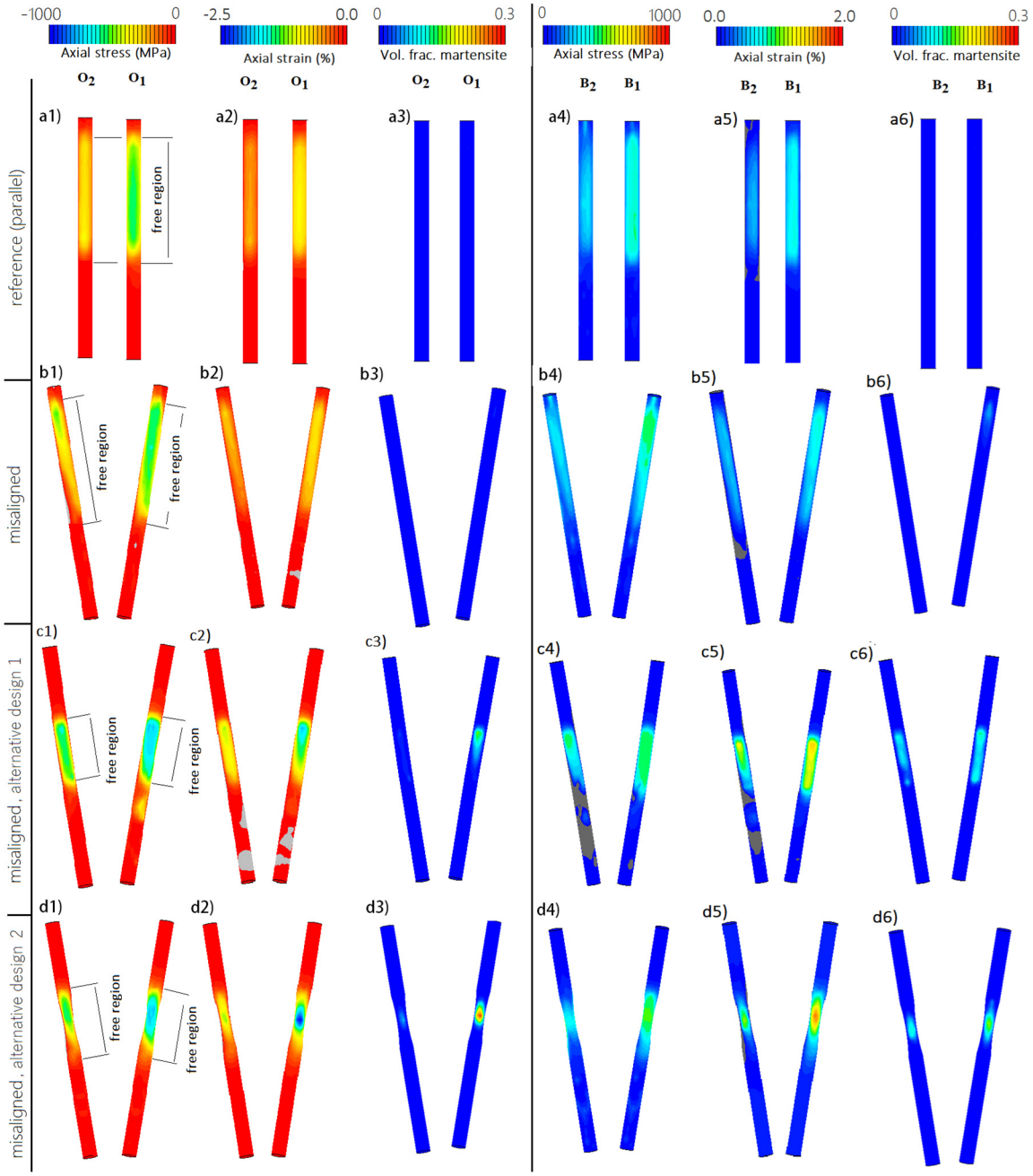

Figure 9. Colormaps of axial stress, axial strain, and martensite volume fraction distribution at NiTi shafts (**a**) reference case study (parallel), (**b**) misaligned, (**c**) misaligned alternative design 1, (**d**) misaligned alternative design 2 (the configurations of the models were outlined in Figure 6). (**a1**–**d1**) compressive stresses at the *Oral Surface*, (**a2**–**d2**) compressive strains at the *Oral Surface*, (**a3**–**d3**) corresponding martensite volume fractions at the *Oral Surface*, (**a4**–**d4**) tensile stresses at *Buccal Surface*; (**a5**–**d5**) tensile strains at the Buccal Surface, (**a6**–**d6**) corresponding martensite volume fractions at the *Buccal Surface*. O_1, O_2, B_1, and B_2 refer to the areas outlined in Figure 7. The NiTi shafts are predominantly under mixed bending and compression, hence, the axial components of non-diagonal Cauchy stress tensor and axial component of the total strain were used for visualization. Note: Gray areas are regions where the magnitude of the presented parameter falls out of the selected range and is negligible.

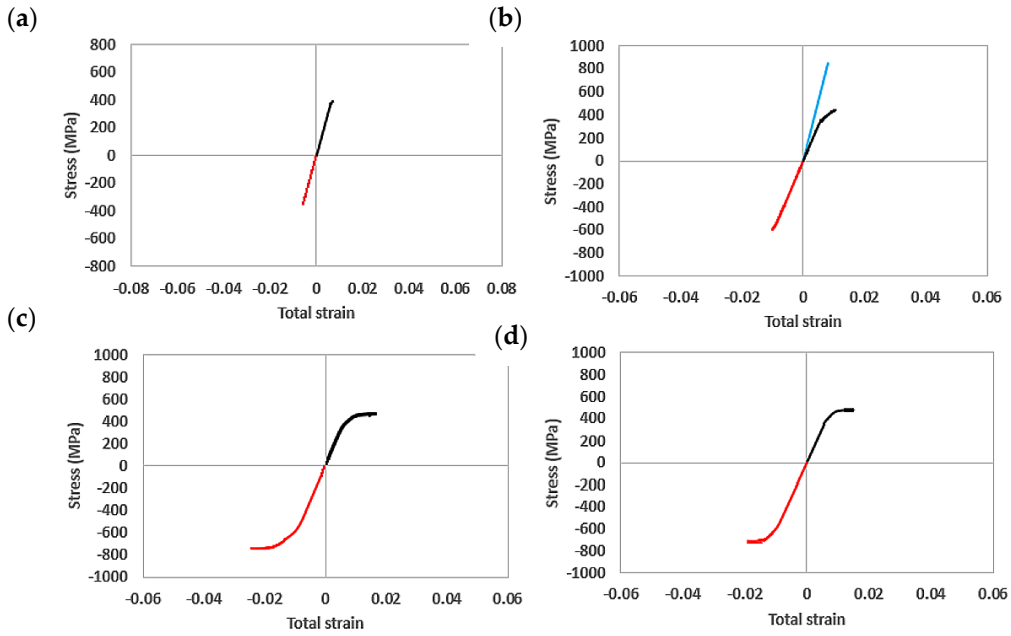

Figure 10. Stress-strain response corresponding to the case studies from Figure 9a–d. (**a**) reference case study (parallel), (**b**) misaligned, (**c**) misaligned alternative design 1, (**d**) misaligned alternative design 2. The data represent points in the *Buccal Surface* (black curve) or the *Oral Surface* (red curve) where the maximum volume fraction of martensite evolves. The blue curve in (**b**) represents the associated response of the case study in which titanium was used instead of NiTi in the misaligned state, for comparative purposes (Figure 11).

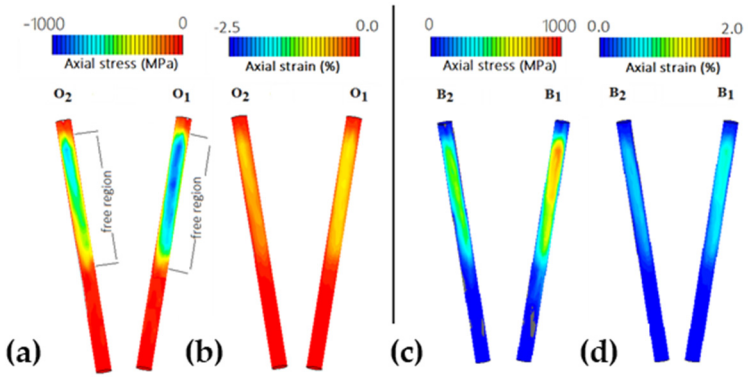

Figure 11. The non-parallel case while using titanium instead of NiTi for the shaft: (**a**,**b**) the compressive stresses and strains at the *Oral Surface*, respectively; (**c**,**d**) the tensile stresses and strains at the *Buccal surface*, respectively. One can compare (**a**–**d**) here, to Figure 9(b1,b2,b4,b5), respectively, where the same state has been presented while using NiTi instead of titanium.

4. Discussion

The results in Figure 9 reveal that in the case of non-parallelism of supporting implants (Figure 9b), the level of induced axial stresses slightly increases at both Oral and Buccal surfaces, as compared to the situation of parallel aligned implants (Figure 9a), which results in higher martensite volume fraction evolution. In the non-parallel state (Figure 9b in comparison to Figure 9a) the stress also (thus, the stress-induced martensite) concentrated in a small region where the male part and shaft were joined (Figure 9(b6)).

To overcome such stress concentrations and thus, very local cyclic phase transitions, alternative design 1 (Figure 5c) was examined in the non-parallel state (Figure 9c). Due to the increase of the contact area between the shaft and male attachment part, the concentration of stress and volume fraction could be reduced, resulting in a larger active transforming

region in the NiTi shaft. To further increase the deformability of the SMA shaft, and to have enhanced control over the location of the maximum stresses for arbitrary misalignments of supporting implants, the second alternative design was tested, where the SMA shaft was necked in the middle (Figure 6d). This minor reduction of shaft diameter triggered higher stress levels at both Oral and Buccal surfaces, which indeed enabled the system to accommodate higher strains at constant stress by the evolution of a higher volume fraction of martensite under an equivalent loading state. The gradual increase of the evolved (compression- and tension-induced) detwinned martensite from the reference geometry to the optimized design number 2, is well illustrated in Figure 10.

Under 150 N vertical force, the maximum stress at both shafts could reach very high values close to the yield point of titanium (~1100 MPa) (stress situation Figure 9(b1) vs. Figure 11a, and Figure 9(b4) to Figure 11c), while the evolved strains were equivalent (strains in Figure 9(b2) vs. Figure 11b, and Figure 9(b5) vs. Figure 11d). Comparing the results in Figure 11a,b and Figure 11c,d with the case represented in Figure 9(b1,b2) and Figure 9(b4,b5), respectively, demonstrated the effectiveness of the application of SMA shafts in the attachment system to accommodate high deformations, whereby the martensitic phase transformation prevented overstressing. The use of SMA potentially also reduced the transmitted (reaction) force to the surrounding implant and bone. To better visualize this effect, Figure 12 compares the reaction stresses on the inner surface of the titanium implants (for a non-parallel state), showing a gradual decrease from the case where the male part was made of titanium to the alternative design 2. This higher reaction force may be seen as a cause for wear phenomena at the male/female interface of current attachment systems. It can be anticipated, that the use of SMA reduces wear phenomena, thereby decreasing maintenance costs [20–23].

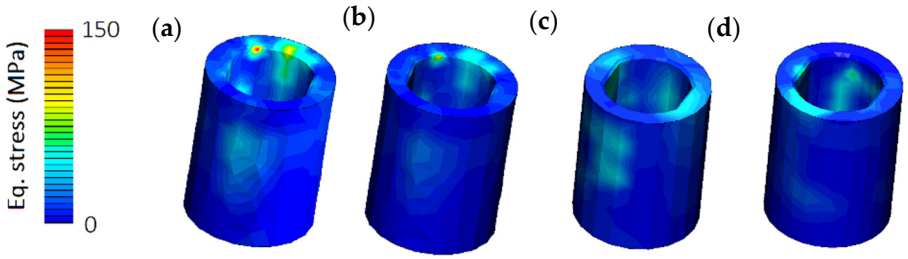

Figure 12. Reaction stresses induced on the inner surface of the titanium implant (implant-abutment interface) for the non-parallel state: (**a**) reference design, male part made of titanium; (**b**) reference design, male part made of NiTi; (**c**) alternative design 1, male part made of NiTi; (**d**) alternative design 2, male part made of NiTi.

Currently, it is not possible to link the simulations carried out to the anticipated clinical performance of the novel attachment system. Given that NiTi is currently being used in dentistry for orthodontic appliances and endodontic instruments [28], the envisaged attachment system requires several additional developmental steps prior to clinical application.

5. Conclusions

Numerical analysis showed that using a superelastic NiTi shaft instead of titanium alloy could result in the ability of the attachment system to withstand large deformations and forces upon masticatory loading while avoiding over-stressing. Moreover, necking the flexible SMA shaft in the middle could prompt better accommodation of large deformations triggered through masticatory loading. An increased contact area between the shaft and the male retentive element of the attachment led to a more favorable, less localized loading situation.

Author Contributions: Conceptualization, M.K.; methodology, M.K., P.S., F.W. and P.H.; software, P.S.; validation, M.K., P.S., F.W. and P.H.; formal analysis, P.S. and F.W.; investigation, M.K., P.S., F.W. and P.H.; resources, M.K. and F.W.; data curation, M.K.; writing—original draft preparation, P.S.;

writing—review and editing, M.K., P.S., F.W. and P.H.; visualization, P.S.; supervision, M.K. and F.W.; funding acquisition, F.W. and M.K. All authors have read and agreed to the published version of the manuscript.

Funding: This research was funded (P.S. and F.W.) by Deutsche Forschungsgemeinschaft (DFG, German Research Foundation)—(DFG—SPP1897 grant WE4747-3/2).

Institutional Review Board Statement: Not applicable.

Informed Consent Statement: Not applicable.

Data Availability Statement: Data are contained within the article. The data presented in this study can be requested from the authors.

Conflicts of Interest: The authors declare no conflict of interest.

References

1. Huang, W.M.; Ding, Z.; Wang, C.C.; Wei, J.; Zhao, Y.; Purnawali, H. Shape memory materials. *Mater. Today* **2010**, *13*, 54–61. [CrossRef]
2. Elahinia, M. *Shape Memory Alloy Actuators: Design, Fabrication and Experimental Evaluation*; John Wiley & Sons: Hoboken, NJ, USA, 2016.
3. Nespoli, A.; Passaretti, F.; Szentmiklósi, L.; Maróti, B.; Placidi, E.; Cassetta, M.; Yada, R.Y.; Farrar, D.H.; Tian, K.V. Biomedical NiTi and β-Ti Alloys: From Composition, Microstructure and Thermo-Mechanics to Application. *Metals* **2022**, *12*, 406. [CrossRef]
4. Es-Souni, M.; Es-Souni, M.; Fischer-Brandies, H. Assessing the biocompatibility of NiTi shape memory alloys used for medical applications. *Anal. Bioanal. Chem.* **2005**, *381*, 557–567. [CrossRef] [PubMed]
5. Maleckis, K.; Anttila, E.; Aylward, P.; Poulson, W.; Desyatova, A.; MacTaggart, J.; Kamenskiy, A. Nitinol Stents in the Femoropopliteal Artery: A Mechanical Perspective on Material, Design, and Performance. *Ann. Biomed. Eng.* **2018**, *46*, 684–704. [CrossRef] [PubMed]
6. Machado, L.G.; Savi, M.A. Medical applications of shape memory alloys. *Braz. J. Med. Biol. Res.* **2003**, *36*, 683–691. [CrossRef]
7. Petrini, L.; Migliavacca, F. Biomedical Applications of Shape Memory Alloys. *J. Metall.* **2011**, *2011*, 1–15. [CrossRef]
8. Dordoni, E.; Petrini, L.; Wu, W.; Migliavacca, F.; Dubini, G.; Pennati, G. Computational Modeling to Predict Fatigue Behavior of NiTi Stents: What Do We Need? *J. Funct. Biomater.* **2015**, *6*, 299–317. [CrossRef]
9. Shayanfard, P.; Šandera, P.; Horníková, J.; Petruška, J.; Šittner, P.; Pokluda, J. Ni-Ti self-expanding vascular stent configuration and biomedical interaction with artery: Finite element analysis. *Solid State Phenom.* **2016**, *258*, 366–369. [CrossRef]
10. Auricchio, F.; Conti, M.; Morganti, S.; Reali, A. Shape memory alloy: From constitutive modeling to finite element analysis of stent deployment. *Comput. Model Eng. Sci.* **2010**, *57*, 225–243.
11. Das, K.P.; Jahangiri, L.; Katz, R.V. The first-choice standard of care for an edentulous mandible: A Delphi method survey of academic prosthodontists in the United States. *J. Am. Dent. Assoc.* **2012**, *143*, 881–889. [CrossRef]
12. Matthys, C.; De Vijlder, W.; Besseler, J.; Glibert, M.; De Bruyn, H. Cost-effectiveness analysis of two attachment systems for mandibular overdenture. *Clin. Oral Implant. Res.* **2020**, *31*, 615–624. [CrossRef] [PubMed]
13. Kleis, W.K.; Kämmerer, P.W.; Hartmann, S.; Al-Nawas, B.; Wagner, W. A comparison of three different attachment systems for mandibular two-implant overdentures: One-year report. *Clin. Implant. Dent. Relat. Res.* **2010**, *12*, 209–218. [CrossRef] [PubMed]
14. Patodia, C.; Sutton, A.; Gozalo, D.; Font, K. Cost and complications associated with implant-supported overdentures with a resilient-attachment system: A retrospective study. *J. Prosthet. Dent.* **2021**, *128*, 181–186. [CrossRef] [PubMed]
15. Brunello, G.; Gervasi, M.; Ricci, S.; Tomasi, C.; Bressan, E. Patients' perceptions of implant therapy and maintenance: A questionnaire-based survey. *Clin. Oral Implant. Res.* **2020**, *31*, 917–927. [CrossRef] [PubMed]
16. Karlsson, K.; Derks, J.; Wennström, J.L.; Petzold, M.; Berglundh, T. Health economic aspects of implant-supported restorative therapy. *Clin. Oral Implants Res.* **2022**, *33*, 221–230. [CrossRef]
17. Jan, D.; Matthys, C.; Sahak, H.; Besseler, J.; Bruyn, H.D. Seven years maintenance cost of implant-retained overdentures on Ball versus Locator ®Abutments. *Preprints* **2020**, *2020*, 110662.
18. Goodacre, C.J.; Bernal, G.; Rungcharassaeng, K.; Kan, J.Y.K. Clinical complications with implants and implant prostheses. *J. Prosthet. Dent.* **2003**, *90*, 121–132. [CrossRef]
19. Goodacre, B.J.; Goodacre, S.E.; Goodacre, C.J. Prosthetic complications with implant prostheses (2001–2017). *Eur. J. Oral Implantol.* **2018**, *11*, s27–s36.
20. Fromentin, O.L.C.; Nader, S.A.; Feine, J.; de Albuquerque, R.F., Jr. Wear of ball attachments after 1 to 8 years of clinical use: A qualitative analysis. *Int. J. Prosthodont.* **2011**, *24*, 270–272.
21. Hahnel, S.; Alamanos, C.; Schneider-Feyrer, S.; Stöckle, M.; Rosentritt, M. Investigation of Clinical and Laboratory Wear in Locator-Supported, Implant-Retained Overdentures. *Int. J. Prosthodont.* **2018**, *31*, 334–337. [CrossRef]
22. Guédat, C.; Nagy, U.; Schimmel, M.; Müller, F.; Srinivasan, M. Clinical performance of LOCATOR®attachments: A retrospective study with 1–8 years of follow-up. *Clin. Exp. Dent. Res.* **2018**, *4*, 132–145. [CrossRef] [PubMed]

23. Matthys, C.; Vervaeke, S.; Besseler, J.; De Bruyn, H. Five-year study of mandibular overdentures on stud abutments: Clinical outcome, patient satisfaction and prosthetic maintenance—Influence of bone resorption and implant position. *Clin. Oral Implant. Res.* **2019**, *30*, 940–951. [CrossRef] [PubMed]
24. Maniewicz, S.; Badoud, I.; Herrmann, F.R.; Chebib, N.; Ammann, P.; Schimmel, M.; Müller, F.; Srinivasan, M. In vitro retention force changes during cyclic dislodging of three novel attachment systems for implant overdentures with different implant angulations. *Clin. Oral Implant. Res.* **2020**, *31*, 315–327. [CrossRef] [PubMed]
25. Passia, N.; Ghazal, M.; Kern, M. Long-term retention behaviour of resin matrix attachment systems for overdentures. *J. Mech. Behav. Biomed. Mater.* **2016**, *57*, 88–94. [CrossRef] [PubMed]
26. Bouhy, A.; Rompen, E.; Lamy, M.; Legros, C.; Lecloux, G.; Lambert, F. Maxillary implant overdenture retained by four unsplinted attachments and opposed by a natural or fixed dentition: One-year clinical outcomes. *Clin. Oral Implant. Res.* **2020**, *31*, 747–767. [CrossRef]
27. Kappel, S.; Klotz, A.L.; Eberhard, L.; Lorenzo Bermejo, J.; Rammelsberg, M.; Giannakopoulos, N.N. Maxillary implant overdentures on two or four implants. A prospective randomized cross-over clinical trial of implant and denture success and survival. *Clin. Oral Implant. Res.* **2021**, *32*, 1061–1071. [CrossRef]
28. Grobecker-Karl, T.; Kafitz, L.; Karl, M. Rationale for a novel attachment system for implant-supported overdentures. *Int. J. Prosthodont.* **2022**, *35*, 74–81. [CrossRef] [PubMed]
29. Prati, C.; Tribst, J.P.M.; Dal Piva, A.M.d.O.; Borges, A.L.S.; Ventre, M.; Zamparini, F.; Ausiello, P. 3D Finite Element Analysis of Rotary Instruments in Root Canal Dentine with Different Elastic Moduli. *Appl. Sci.* **2021**, *11*, 2547. [CrossRef]
30. Choudhry, S.; Yoon, J.W. A General Thermo-Mechanical Shape Memory Alloy Model: Formulation and Applications. *AIP Conf. Proc.* **2004**, *712*, 1589–1594.
31. Shayanfard, P.; Heller, L.; Šandera, P.; Šittner, P. Experimental and Numerical Investigation of Thermomechanical Cycling of Notched NiTi Shape Memory Ribbon Using SMA Model Accounting for Plastic Deformation. *J. Mater. Res. Technol.* **2021**, *15*, 1759–1776. [CrossRef]
32. Reedlunn, B.; Churchill, C.B.; Nelson, E.E.; Shaw, J.A.; Daly, S.H. Tension, compression, and bending of superelastic shape memory alloy tubes. *J. Mech. Phys. Solids* **2014**, *63*, 506–537. [CrossRef]
33. Mirzaeifar, R.; Desroches, R.; Yavari, A.; Gall, K. On superelastic bending of shape memory alloy beams. *Int. J. Solids Struct.* **2013**, *50*, 1664–1680. [CrossRef]
34. Kikuchi, M.; Takahashi, M.; Okuno, O. Elastic moduli of cast Ti-Au, Ti-Ag, and Ti-Cu alloys. *Dent. Mater.* **2006**, *22*, 641–646. [CrossRef] [PubMed]